UNIVERSAL LASER-PULSE APPARATUS FOR THERMOPHYSICAL MEASUREMENTS IN REFRACTORY MATERIALS AT VERY HIGH TEMPERATURES

C. Ronchi, W. Heinz, M. Musella, and R. Selfslag
European Commission, Joint Research Centre
Institute for Transuranium Elements, Karlsruhe, Germany
M. Sheindlin
High-Energy Density Research Centre, Moscow, Russia

ABSTRACT

The paper presents a new experimental set-up developed in the JRC-ITU laboratory, enabling thermophysical measurements to be carried out at very high temperatures in a very simple and small pressurised vessel in which the sample is heated by a continuous wave laser, and subsequently submitted to a short temperature pulse. The adopted method is essentially an extension of the "Laser-Flash" technique, widely used for thermal diffusivity measurements, whereby, in addition, the heat capacity - and hence the thermal conductivity, l , are simultaneously evaluated from the pulse analysis. Applications are presented on thermal diffusivity and heat capacity of graphite, zirconia and uranium dioxide up to temperatures above *3000K.*

KEY WORDS: heat capacity ; high-speed pyrometry; laser flash ; laser heating, poco graphite ; thermal conductivity ; thermal diffusivity; uranium dioxide.

1. INTRODUCTION

The idea of measuring the heat capacity of a sample from the temperature increase produced by an applied energy pulse of known intensity dates from 1961 when *Parker et al.* published the first paper /1/ on the *flash-method* for thermal diffusivity measurements. Yet, the sub-second instrumentation available at that time was so unsophisticated, that this was seen as a merely virtual possibility. Though, with progress of laser technology and fast pyrometry, the *flash-method* became more and more precise, for

nearly three decades any extension of this technique to calorimetric measurements was considered impracticable. Only at the end of the 80's, in the *Institute of Technology* of the *Jet Propulsion Laboratory, Pasadena (Ca),* a flash-method was successfully applied, using a Xenon lamp, for heat capacity measurements up to *1300 K* /2/. The method was, however, based on a comparative empirical procedure, moreover, the sample had to be sputtered with graphite in order to ensure a constant absorbivity. The weak point of this set-up was the sensitivity of the measurements to sample positioning within the light beam. In 1990, in the *National Laboratory of Metrology, Ibaraki (Japan),* a feasibility study was positively concluded, in which a laser-flash device was used to measure heat capacity /3/. Again, a comparative method was chosen, whereby, this time, in order to avoid misalignments, the standard sample was permanently mounted in a separate holder, and was thus acting as a rudimentary reference calorimeter.

A new experimental set-up was recently constructed in our laboratory, using advanced pyrometric techniques in conjunction with high quality lasers beams (obtained by optical fibers) and optical diagnostics equipment. An absolute calorimetric method was implemented, in which the maximum useful amount of experimental information is exploited to simultaneously obtain thermal diffusivity and heat capacity up to very high temperatures, and with a good accuracy. Furthermore, with the same set-up a very accurate determination of the phase transition parameters can be obtained with a precision of better than *1K* - this aspect is, however, not treated in this paper.

2. MEASUREMENT PROCEDURE

The apparatus is schematically shown in Fig.1. The sample, a disk of *5 mm* diameter and $\approx$ *0.5 mm* thickness, is held by a three-pin mounting in a small autoclave. Two opposite *CW Nd-YAG* laser beams (of *300 W* total power) heat the two faces of the sample up to the conditioning temperature. This is recorded on both faces of the disk by two rapid and precise pyrometers (*settling time to 1% = 10*μ*s* , *sensitivity* $<$ *0.1K*).

Thanks to the almost flat radial profile of the laser beam power in the focal spot (of *5mm* diemeter), and to its stability in time, a homogeneous and constant surface temperature can be rapidly achieved within the illuminated spot. A temperature pulse of *1-2 ms* duration and less than *0.5 J* energy is then deposited onto the front face of the sample with a *YAG* laser. The front-face temperature rise is detected

above the steady-state level, while a similar pyrometer is viewing a spot of *0.3 mm* diameter on the rear face of the sample. Their signals are sent to a *14-bit* A/D converter, providing a detection accuracy of better than *0.05K*. The pulse power is measured as a function of time by a *Si*-photodiode, which collects a fixed fraction of the laser beam. The integral energy collected by the photodetector is calibrated with a disk calorimeter (SCIENTEC, precision: 3%). The deposited surface power is calculated from the optical absorbivity of the sample at the wavelength of the *Nd-YAG* laser, measured with an integrating sphere reflectometer with a precision of better than 5%. Finally, the probe-beam spatial profile in the focal point is measured, through a beam splitter, by a CCD camera.

3. ANALYTICAL

In the new apparatus, the homogeneity and symmetry of the heating conditions, in conjunction with the high precision and sensitivity of the instruments enable sophisticated thermal diffusivity measurements to be performed (see /4/ for details). In this paper, it will be shown how the thermal diffusivity, a, and the heat capacity, C_p, can be simultaneously evaluated. The method is based on fitting the measured temperatures by the integral of the pulse diffusion equation, $\Delta T = \Delta T(t, \{C_p, a\})$, obtained for sufficiently realistic boundary conditions. This problem, which was investigated in the context of the thermal diffusivity measurements, presents serious difficulties when large heat losses - unavoidable at high temperatures - or spatial variations of the deposited power density are present during the shot.

The adopted fitting function represents the general case of a pulse propagation into a platelet with the sole restriction of preserved cylindrical symmetry: for a disk of density ρ with axial co-ordinates $0 \le z \le l$ and radial co-ordinates $0 \le r \le R$, this function is approximated by the product of the pulse propagation function in an infinite slab of thickness l, and the radial propagation of a cylindrical surface source at $z=0$ of total energy Q, deposited with time dependence $\varphi(t)$ and radial dependence $f(r)$:

$$\Delta T(x,r,t) = \frac{2}{\pi l^2 \rho C_p} \frac{Q}{\tau} \sum_{n=1}^{\infty} \frac{\alpha_n \left(2\alpha_n^n + Y_2^2\right)\left(\alpha_n \cos\alpha_n z + Y_1 \sin\alpha_n z\right)}{\left(\alpha_n^2 + Y_1^2\right)\left(\alpha_n^2 + Y_2^n + Y_2\right) + Y_1\left(\alpha_n^2 + Y_2^2\right)} \times \tag{1}$$

$$\times \int_0^t \varphi(t') \sum_{j=1}^{\infty} \exp(-a\lambda_j^2 t') \frac{J_0(r\lambda_j)}{J_0^2(R\lambda_j) + J_1^2(R\lambda_j)} \int_0^R r' f(r') J_0(r'\lambda_j) \exp\left(\frac{-\alpha_n^2}{l^2} a t'\right) dr' dt'$$

where α_n and λ_n $(n = 1 \ldots \infty)$ are, respectively, the roots of the equations:

$$\left(a^2 - Y_1 Y_2\right) tg(a) = a\left(Y_1 + Y_2\right); \qquad Rl\, J_1(Rl) = Y_r J_0(Rl)$$

and Y_1, Y_2, Y_r are, respectively, the Biot numbers on the front ($z = 0$), rear ($z = 1$) and lateral ($r=R$, $z=l/2$) surface of the sample. Finally, function (1) depends on the five parameters: a, C_p, Y_1, Y_2, Y_r. The experimental temperature function, $T_{exp}(t)$, is fitted with integral (1), by varying *all* or *some* of these parameters.

A five-parameter fitting is only practicable if a fitting strategy is applied, based on the hierarchical rank of the variables. In fact, the thermal diffusivity, a, is by far the most influential parameter, followed by C_p and the *total* heat-loss; whilst the partition of this latter into the three "top", "bottom" and "radial" directions represents a third rank variable. Fitting is, therefore, started with the variables of the first and second rank, those of third rank being previously assessed - for instance by calculation of the ratios of Y_2 and Y_r to Y_1. A further optimisation of the latter parameters can only follow if the N-dimensional non-linear fitting (with $N \leq 5$) sufficiently provides "robust" solutions in the sense explained below[1]. This condition depends mainly on the extent, range and quality of the specific experimental database.

For M measurements, the minimum of the sum $F = \sum_{m=1}^{M} f_m^2$, is sought, where: $f_m = \left[\, 1 - T(r, t_m, \bar{x}) / T_{\exp} \,\right]$ and $\vec{x} = \left\{x_1, x_2, x_3, x_4, x_5\right\} = \left\{a, C_p, Y_1, Y_2, Y_r\right\}$. The goodness of fitting is first given by the attained minimum value of F, and by the *statistical distribution* of the deviations f_m. In *linear* regression applications this aspect can be rigorously treated. In *non-linear* regression, however, the problem is much more complex. In fact, a statistical error analysis is only feasible if function F in the vicinity of its absolute minimum is linear in $\vec{x}$, or, at least, sufficiently regular with respect to continuity and derivability to allow an expansion into a rapidly converging Taylor's series. In this case, a N x N covariance matrix $\|b\|$ can be defined and calculated in analogy with the linear regression method, by the terms:

$$b_{rs} = \sum_{m=1}^{M} \frac{\partial T_m}{\partial x_r} \frac{\partial T_m}{\partial x_s} \qquad (2)$$

The variance of the fitted parameter of index i, is then expressed as:

[1] Obviously, if one additional variable is introduced, *all* fitting variables are simultaneously re-calculated.

$$= s \sqrt{\frac{M}{M-N}\frac{B_{ij}}{B}}, \qquad (3)$$

where B is the determinant of $\|b\|$, B_{ii} is the cofactor of the element b_{ii}, and:

$$s' = \sqrt{\left(\frac{1}{M}\sum_{m=1}^{M} f_m^2\right)} \qquad (4)$$

is the MSQ residual fitting error. An insight into eq.(3) reveals that, by increasing the number of fitting parameters, N, (and, hence, the rank of the determinant B) the precision of *all* the fitted parameters is affected; and whilst s' obviously decreases by increasing N, nothing can be said *a priori* on the behaviour of the fraction in the square root of eq.(3). In practice, with an experimental error of $\Delta T \leq 1\%$ a significant fitting of five parameters can be obtained if s' is of the order of 0.5% or less . In our best experiments we obtained $s_{Cp} \approx 3\%$, $s_a \approx 0.5\%$, $s_{Y1,Y2,Yr} \approx 10\%$. However, in most cases a precision $s_{Cp} < 5\%$ can also be obtained by fitting only three parameters, including the sum of the heat losses, and a previous reasonable estimation of the ratios of the Biot numbers, Y_j.

4. HEAT CAPACITY AND DIFFUSIVITY MEASUREMENTS

4.1. *GRAPHITE*

POCO -5Q AMX graphite was measured as a reference material up to *3200K*. The best literature data (up to *2400K)* were obtained with the *direct electrical heating* technique. Fig.2 shows our results compared with these data. It can be seen that in the common temperature range our measurements differ from the others by approximately 5%, whereby our error is 8%. It should be, however, remarked that our points correspond to individual measurements obtained from single shots, whilst, for instance, for the thermal conductivity the three rows of points of *Taylor & Groot* respectively represent measurements on three nominally identical samples.

4.2. *URANIUM DIOXIDE*

Since this material markedly vaporises at $T > 2000K$, thermophysical measurements at high temperatures are rather difficult. The very short duration of our measurements is, therefore, of great advantage. In fact, the samples, stoichiometric ($10.5\ gcm^{-3}$ dense) sintered pellets, did *not* show after the measurements in

Ar:2%H_2 significant vaporisation or stoichiometry variations up to *2600K* (post-measurement *O/U=1.995*). The results are plotted in Fig.3. Measurements above *2600K* are still in progress with a different laser pulse duration. The thermal diffusivity, in spite of a dramatic restructuring of the sample, exhibits a monotonic *decrease* up to *2500K*; at higher *T* the slope is significantly smaller. Particularly interesting are the measurements of the thermal conductivity: after a pronounced decreasing stage at low temperatures, λ increases weakly in the interval *2000-2600K*. The trend of $\lambda(T)$ at high temperature seems to exclude a large increase of this quantity in the temperature interval preceding melting (*3150 K*), indicating a closer approach to the value of λ in the liquid /12/ than predicted by the extrapolating curves of *Fink et al* . /10/ and *Hyland* /11/.

The measured heat capacity points lie within $\pm$5% on the curve, reported in ref. /10/, obtained by differentiating the enthalpy measurements of *Hein & Flagella*. Noteworthy is the large scatter of the data above 2500K, probably due to the vicinity of the pre-melting transition /16/, which starts affecting the front-surface layer.

4.3. *ZIRCONIA*

Cubic-stabilised ZrO_2:20%Y_2O_3 was measured. The samples were fabricated by plasma spraying with a macroscopic density of $5.07\ gcm^{-3}$. The (textured) sintered porosity proved to be stable up to circa *2500K*, though a permanent increase in thermal diffusivity is detected after heating above *1500 K*, probably due to healing of lattice defects and grain boundary restructuring. No changes in stoichiometry or colour were observed after the measurements. While the sample is white at room temperature, above *1800K* it sufficiently exhibits a high and stable absorbivity (> 0.65 measured at *1060 nm)* to enable steady state temperature fluctuations of $< -1K$ to be achieved. The results for heat capacity are plotted in Fig.4. As for the thermal diffusivity, whose above mentioned thermal recovery is here matter of little interest, it can be seen that between *1850K* and *2800K* is in the interval $4.2 - 0.5\ cm^2/s$, increasing weakly with temperature. In the same *T* interval, the measured heat capacity increases only from *620 to 700* $J\ Kg^{-1}K^{-1}$. The observed behaviour of C_p has, however, important physical implications. In fact, in analogy with other *f.c.c.* ionic dioxides, a marked increase of the heat capacity at high temperatures is normally expected, due to formation of oxygen Frenkel pairs, a thermal process in which a large energy

is spent. The existing literature data are in disagreement: on one hand, *Pears* /13/ in his samples (*1% Ca*-stabilised, supplied by *Zirconium Corp. of America*, whereby after exposure at high temperature both the oxygen-to-metal ratio and the *Ca*-content decreased) measured a marked upswing of C_p above *2000K*, corroborating the hypothesis of substantial oxygen defect formation at high temperatures; on the other hand, the measurements of *Chekhovskoy et al.* /14/ on *pure, non-stabilised* zirconia exhibit a weak dependence of C_p on T up to *2750K* and *no composition changes*. Our measurements - on a doped, but chemically stable material - are in agreement with the latter data. This should confirm that stoichiometric stability reduces intrinsic Frenkel defect formation. In fact, creation of oxygen Frenkel pairs requires a local charge re-arrangement which is improbable in compounds like pure ZrO_2, where all cations have a fixed valence (see, for instance, the analogous behaviour of ThO_2 /15/). On the other hand, in oxides where a valence disproportioning is possible - like e.g. UO_2- oxygen defect concentration attains at sufficiently high temperatures fractional concentrations of the order of magnitude of 10^{-1}, producing a marked increase in C_p /16/. As for the effect of yttrium doping, literature data /17/ indicate that in Y_2O_3 the curve $C_p(T)$ reaches a plateau above *1600K* at C_p/R @*15*, a value corresponding to the saturation of the vibrational modes of a *penta*-atomic crystal. Now, according to our data, the heat capacity in yttria-doped ZrO_2 above *1800K* stabilises at C_p/R @*9*, i.e. the saturation value of a *tri*-atomic lattice. Since yttrium doping maintains C_p near to the value corresponding to the perfect lattice of ZrO_2, one can infer that the extrinsic excess oxygen of yttria indeed inhibits thermal Frenkel pair formation. Though perfectly plausible, these conclusions - which may be important for the refractory properties of the various types of zirconia - leave out of consideration the underlying dependence on dopant concentration of the effective free energy and entropy of formation of defects in the lattice, an aspect which may entail unexpected dramatic changes in the temperature dependence of C_p (see e.g. /16/). Therefore, extrapolations of these results to other types of stabilised zirconia must be considered with care.

5. CONCLUSIONS

It has been shown that the new laser-flash device, presented in the paper, can be used for *simultaneous* and *consistent* measurements of heat capacity and thermal diffusivity, enabling a reliable insight into the

effectively ruling heat transport mechanisms to be obtained. This is typically shown by the discussed measurements in UO_2 and ZrO_2.

6. REFERENCES

/1/ W.J. PARKER, R.J. JENKINS, C.P. BUTLER, and G.L. ABBOT, Journ. Appl. Phys. 32, **9,** 1679 (1961)

/2/ J.W. VANDERSANDE, A. ZOLTAN, and C. WOOD, Int. Journ. of Thermophys. 10, **1,** 251 (1989)

/3/ T. BABA, Proc. 11th Japan Symp. on "Thermophysical Properties" Tokyo, Nov. 6-8, p. 449 (1990)

/4/ C. RONCHI and M. SHEINDLIN , submitted to Rev. Sci. Instr.

/5/ T.BABA and A.CEZAIRLYIAN, Int. Journ. of Thermophys. **15,** 343 (1994)

/6/ R. TAYLOR, and H. GROOT, High Temp.-High Press. **12,** 147 (1980)

/7/ A. CEZAIRLIYAN, F. RIGHINI, Rev. Int. Hautes Temp. Refract. **12,** 124 (1975)

/8/ G.A. BERGMAN et al., State Bureau of Standard Reference Data GSSSD 25-90,USSR Committee of Quality of Products, Moscow (1991)

/9/ J.-C. WEILBACHER, High Temp.-High Press. **4,** 431 (1972)

/10/ J.K. FINK, M.G. CHASANOV and L.LEIBOWITZ, Journ. Nucl. Mater. **102,** 17 (1981)

/11/ G.J. HYLAND, Journ. Nucl. Mater. **113,** 125 (1983)

/12/ H. A. TASMAN, Report EUR 12385, European Commission JRC (1989)

/13/ C.D. PEARS, U.S. Report ASD-TDR 62-765 1-420 (AD 298 061) (1963)

/14/ V.Y.CHEKHOVSKOY, V.Y.ZUKHOVA, and V.D.TARASOV, Tepl. Vys.Temp. 17, **4,** 54 (1979)

/15/ C. RONCHI, and J.P. HIERNAUT, Journ. Alloys and Comp. **240,** 179 (1996)

/16/ C. RONCHI, and G.J. HYLAND, Journ. Alloys and Comp. **213/214,** 159 (1994)

/17/ L.B. PANCRATZ, E.G.KING, and K.K.KELLEY, US Bur. Mines, Rept.Invest., **6033** , 1 (1962)

7. CAPTIONS OF THE FIGURES

Fig.1: Scheme of the set-up for thermal diffusivity and heat capacity measurements.

Fig.2: Thermal diffusivity, heat capacity and conductivity of graphite. The curves respectively refer to: **1**: *ITU conventional laser-flash measurement in a furnace*; **2:** *this work*; **3:** *Maglic reported in ref.* /5/; **4:** *ref.* /5/; **5**: *ref.* /6/; **6:** *this work* ; **7:** *ref.* /7/; **8:** *ref.* /8/; **9:** *this work*; **10:** *ref.* /6/. The literature heat capacity values correspond to fitting spline functions - whence the good alignment of the respective points - whilst our points represent single, direct measurements. The same yields for the thermal conductivity, whereby in this case the data by *Taylor & Groot* represent different smoothed curves obtained from three different samples.

Fig.3: Heat capacity, thermal diffusivity and thermal conductivity of UO_2. **1:** *this work*; **2:** *ref.*/10/; **3:** *this work* ; **4:** *ref.* /9/; **5:** *this work* ; **6:** *linear fitting of curve* ***5;*** **7:** *ref.* /10/; **8:** *ref.* /11/.

Fig.4: Zirconia heat capacity as a function of temperature: **1:** *ref.* /13/; **2:** *ref.* /14/; **3:** *this work, points and linear fitting*. The measurements by *Pears* /13/ and *Chekhovskoy* /14/ are obtained by differentiating a spline curve of enthalpy vs. temperature. The zirconia used by *Chekhovskoy* was not stabilised, and, consequently a discontinuity in C_p is found at the tetragonal-cubic phase transition at T @ $1450K$.

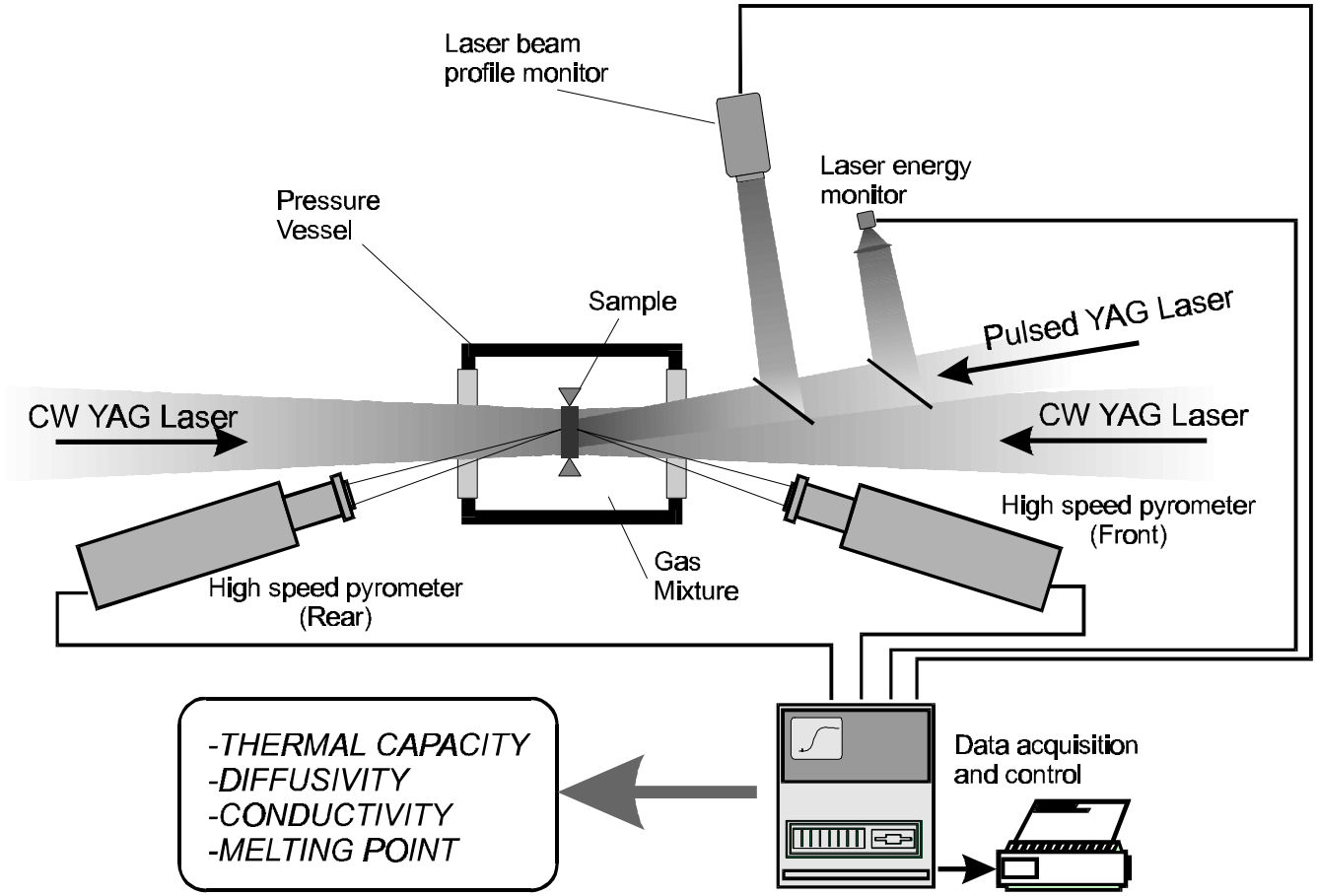
Laser beam
profile monitor
Laser energy
monitor
Pressure
Vessel
Sample
Pulsed YAG Laser
CW YAG Laser
CW YAG Laser
High speed pyrometer
(Front)
Gas
Mixture
High speed pyrometer
(Rear)
-THERMAL CAPACITY
-DIFFUSIVITY
-CONDUCTIVITY
-MELTING POINT
Data acquisition
and control

Fig.1

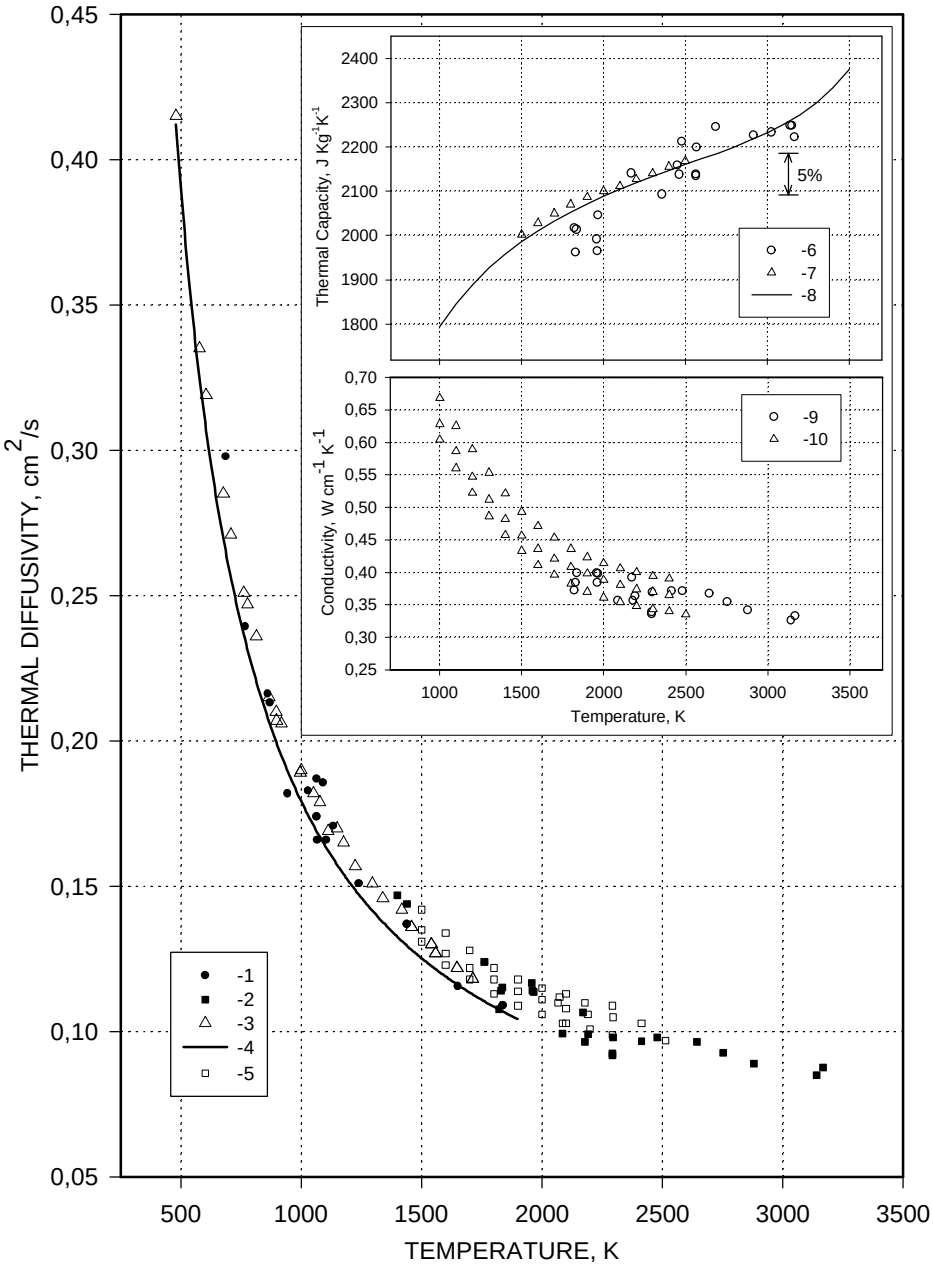
THERMAL DIFFUSIVITY, cm2/s
TEMPERATURE, K
-1
-2
-3
-4
-5
Thermal Capacity, J Kg-1K-1
5%
-6
-7
-8
Conductivity, W cm-1 K-1
-9
-10
Temperature, K

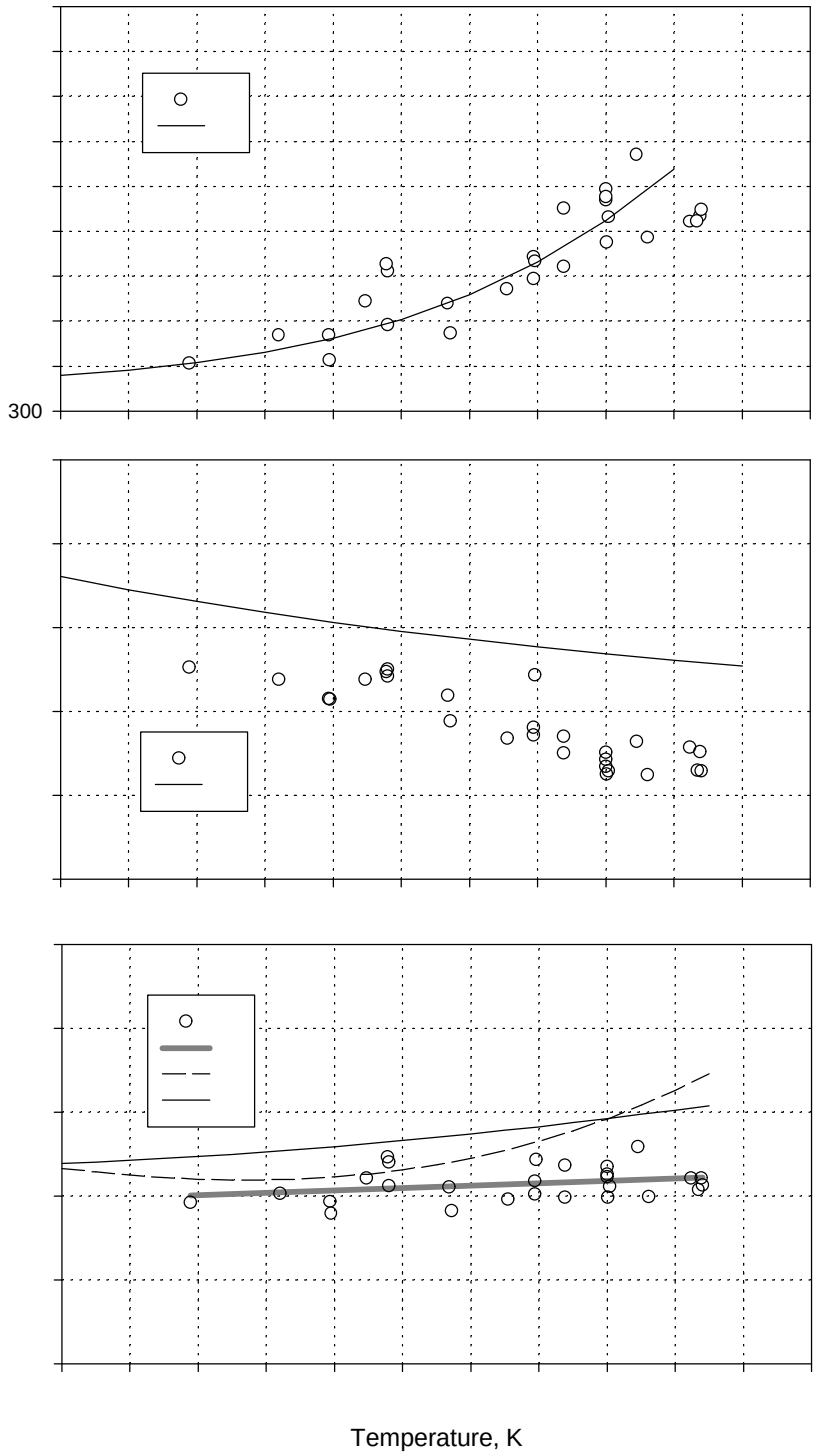

Fig.3

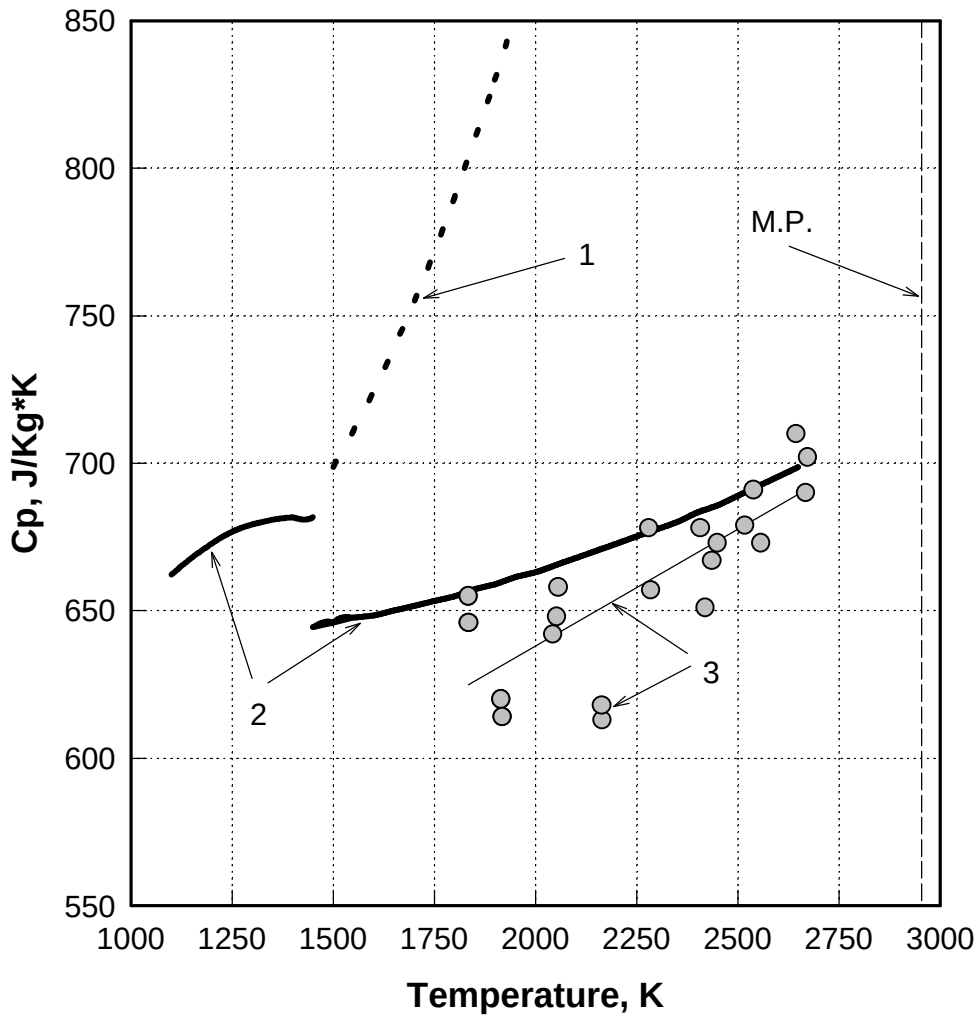
850
800
750
700
650
600
550
1000
1250
1500
1750
2000
2250
2500
2750
3000
Cp, J/Kg*K
Temperature, K
M.P.
1
2
3

Fig.4